Kinetic Study of the External Heavy-Atom Quenching of Fluorescence in Liquid Solution under High Pressure

Masami Okamoto

Faculty of Engineering and Design, Kyoto Institute of Technology, Matsugasaki, Sakyo-ku, Kyoto 606-8585, Japan

Received: February 10, 2000; In Final Form: May 9, 2000

The rate constants, k_q, for the fluorescence quenching of pyrene by six heavy-atom quenchers, carbon tetrabromide (CBr_4), pentabromoethane (PENTBE), 1,2-tetrabromoethane (TETRBE), 1,1-dibromo-2-bromoethane (TRIBE), 1,2-dibromoethane (DIBE), and bromoethane (BE), were measured in methylcyclohexane (MCH) at pressures of up to 650 MPa and 25 °C. The plots of ln k_q against pressure show a monotonical decrease for CBr_4 and PENTBE, a maximum for TETRBE and TRIBE, and a monotonical increase for DIBE and BE. The activation volumes were estimated as 18.9, 12.0, −10.2, −8.0, −7.3, and −7.1 cm^3/mol for CBr_4, PENTBE, TETRBE, TRIBE, DIBE, and BE, respectively. For CBr_4 and PENTBE, the plots of $1/k_q$ against η, where η is solvent viscosity, were approximately linear with positive intercepts, whereas for TETRBE, TRIBE, DIBE, and BE, they deviated significantly from linearity. These results are interpreted to occur by a quenching mechanism via an encounter complex formed between the singlet state of pyrene and heavy-atom quencher molecules, which is followed by exciplex formation in the solvent cage. It was shown that the ratio k_{diff}/k_{-diff}, of the rate constant for the formation (k_{diff}) to that for the dissociation (k_{-diff}), of the encounter complex involved in the kinetic model increases with increasing pressure, and also that the pressure dependence of k_{diff}/k_{-diff} is described satisfactorily by the radial distribution function at the closest approach distance between the solute molecules. From these facts, together with the finding that k_{diff} is approximately inversely proportional to the solvent viscosity, the pressure dependence of k_q observed in this work was attributed to the competing rate processes of the bimolecular quenching constant, k_{bim}, with k_{diff}.

Introduction

The addition of compounds with heavy atoms, such as bromine and iodine, to a solution of fluorescent substance leads to the decrease of both fluorescence intensity and lifetime. This phenomenon is attributed to increased intersystem crossing induced by the interactions between the fluorophore and heavy-atom quencher molecules in deactivation.[1] The quenching rate constant, k_q, varies from diffusion controlled to kinetically controlled depending on the heavy-atom quencher.[2−9] The fact that k_q changes in a wide range has been interpreted by assuming an exciplex, (MQ)*, that is formed reversibly between the fluorophore (^{1}M*) and heavy-atom quencher (Q) molecules, although no emission characteristics of an exciplex have been observed.[2−7] For strong quenchers, such as carbon tetrabromide, the quenching is nearly diffusion controlled as a result of the faster deactivation of (MQ)* compared with the dissociation.[2−6,8,9] For weak quenchers, such as carbon tetrachloride, on the other hand, the dissociation is much faster than deactivation so the quenching is less than the diffusion rate.[2,4−7]

A few high-pressure studies on the fluorescence quenching by some heavy-atom quenchers have been reported.[10−13] Recent work[13] revealed that the rate constant, k_q, for the fluorescence quenching by carbon tetrabromide of pyrene and 1,2-benzanthracene decreases significantly with increasing pressure at pressures up to 400 MPa. From the analysis of pressure-induced solvent viscosity dependence of k_q, it was concluded that the quenching is diffusion controlled at the higher-pressure region, but is competing with the diffusion processes at 0.1 MPa. The present work is focused on the pressure dependence of the fluorescence quenching of pyrene by heavy-atom quenchers with k_q from $\sim 10^6$ to 10^{10} M^{-1} s^{-1} at 0.1 MPa to obtain further insight into the quenching mechanism in liquid solution.

The lifetime of singlet oxygen in liquid solution decreases moderately with increasing pressure.[14,15] The reduction in the lifetime is not only due to the increase in the concentration of solvent but also to the increase in the collision frequency between the singlet oxygen and solvent molecules at high pressure, which is caused by the decrease in free volume. Consequently, the pressure dependence of the lifetime was satisfactorily interpreted from the pressure dependence of the value of the radial distribution function at the closest approach distance of the solute and solvent molecules. This approach was successfully applied to systems with charge transfer (CT) interactions between singlet oxygen and donor pairs.[16−19] For the quenching of singlet oxygen with lifetimes of microseconds, the quenching does not compete with the diffusion processes even at high pressures of a few hundred megapascals. However, for the systems investigated in the present work, it is necessary to take into account the contributions to k_q of the diffusion processes as well as of the collision frequency in liquid solution.

The rate constant for diffusion-controlled reactions, k_{diff}, is often expressed by the Debye equation in a continuum medium with viscosity, η,[20,21]

$$k_{diff} = 8RT/\alpha\eta \qquad (1)$$

where α is 2000 and 3000 for the slip and stick boundary limits, respectively. However, the expression of eq 1 has often failed.

10.1021/jp000535e CCC: $19.00
Published on Web 07/21/2000

TABLE 1: Melting Points, T_{mp}, Boiling Points, T_{bp}, van der Waals Radii, r_W, and a Microfriction Factor, f^{SW}, defined by Spernol and Wirtz for the Solute and Solvent Molecules

				f_i^{SW}[b]	
molecule	T_{mp}, K	T_{bp}, K	r_W, nm[a]	trunc	full
MCH	147	374	0.304	0.560	0.560
PY	429	677	0.351	0.622	0.808
PENTBE	329	573	0.321	0.582	0.698
TETRBE	273	517	0.306	0.563	0.642
TRIBE	244	461	0.289	0.540	0.597
DIBE	283	405	0.270	0.515	0.585
BE	154	312	0.248	0.486	0.456
CBr_4	367	463	0.289	0.541	0.727

[a] Estimated values by the method of Bondi.[28] [b] See text.

This failure may be mainly attributed to the neglect of the difference in size of the solute and solvent molecules and also to the deviation from the continuum model that arises as a result of short-range interactions between the solute and solvent molecules, such as translational and rotational coupling. An empirical equation developed by Spernol and Wirtz,[22,23] for which α in eq 1 is replaced by α^{SW} that depends on the properties of the solvent and solute molecules, has been applied successfully to diffusion-controlled radical self-termination reactions,[24] exothermic triplet excitation transfer,[25−27] and exciplex formation reactions.[13] In this work, the rate constant for diffusion, k_{diff}, is estimated by analysis of the pressure dependence of k_q, followed by the evaluation of α in eq 1, and α^{ex} thus determined is compared with α^{SW}.

Finally, in the present work, the fluorescence quenching of pyrene by heavy-atom quenchers was investigated to understand the pressure effect on fast chemical reactions in liquid solution. For this purpose, the quenching experiments were carried out at pressures of up to 650 MPa for five polybromoethanes in methylcyclohexane because the quenching ability can be changed by changing the number of bromine atoms incorporated in the quencher. The properties of solvent and solutes that are necessary for the analysis of the data are shown in Table 1, in which van der Waals radii, r_W, were estimated by the method of Bondi.[28]

Experimental Section

Pyrene (PY) (Wako Pure Chemicals Ltd.) of guaranteed grade was chromatographed twice on silica gel (200 mesh), developed and eluted with pentane, and then recrystalized from ethanol. Carbon tetrabromide (CBr_4; Wako Pure Chemicals Ltd.) of guaranteed grade was purified by sublimation twice under reduced pressure. Pentabromoethane (PENTBE), 1,2-tetrabromoethane (TETRBE), 1,1-dibromo-2-bromoethane (TRIBE), 1,2-dibromoethane (DIBE), and bromoethane (BE; Tokyo Kasei Kogyo Company, Ltd.) were used without further purification. Methylcyclohexane (MCH) of spectroscopic grade (Dojin Pure Chemicals Company) was used as received.

Fluorescence decay curve measurements at high pressure were performed using a 0.3-ns pulse from a PRA LN103 nitrogen laser for excitation. The fluorescence intensity was measured with a Hamamatsu R1635−02 or R928 photomultiplier through a Ritsu MC-25N monochromator, and the resulting signal was digitized with a Hewlett-Packard 54510A or a Lecroy 9362 digitizing oscilloscope. All data were analyzed with a NEC PC-9801 or a NEC PC-9821 microcomputer, which was interfaced to the digitizers. The details about the associated high-pressure techniques have been described elsewhere.[12]

The concentration of PY was adjusted to $\sim 7 \times 10^{-6}$ M, where the excimer formation is neglected. The sample solution was deoxygenated by bubbling nitrogen gas under nitrogen atmosphere for 20 min. For the quenching in BE, the bubbling was carried out at 0 °C because of the low boiling point. The change in the concentration of the quencher by bubbling was corrected by weighing the sample solution. The increase in the concentration due to the application of high pressure was corrected by using the compressibility of solvent.[29−31]

Temperature was controlled at 25.0 ± 0.2 °C. Pressure was measured with Minebea STD-5000K strain gauge or a calibrated manganin wire.

Results

The fluorescence decay curve in the absence of the quencher was analyzed satisfactorily with a single-exponential function under all the experimental conditions examined. The values of the decay constant, k_M, are listed in Table 2, together with the data of solvent viscosity, η.[29−31] The values of k_M at pressures of up to 400 MPa are in good agreement with those reported previously.[32]

Decay curves of fluorescence in the presence of the quencher, Q, was measured as a function of the concentration of Q, [Q], at pressures of up to 650 MPa, and found to be single exponential for all the experimental conditions examined. The quenching rate constant, k_q, was determined by the least-squares

TABLE 2: Quenching Rate Constant, k_q, in MCH

			$k_q/10^9$ M^{-1} s^{-1} [b]					
P, MPa	η, 10^{-2} P	k_M, 10^6 s^{-1} [a]	CBr_4[c]	PENTBE	TETRBE	TRIBE	DIBE	BE[d]
0.1	0.674	2.48	11.70	7.57	0.262	0.0354	0.0135	0.00278
50	1.143	2.54	7.55	5.49	0.303	0.0400	0.0149	0.00305
100	1.739	2.56	5.14	4.28	0.335	0.0430	0.0163	0.00331
150	2.542	2.58	3.63	3.18	0.358	0.0465	0.0176	0.00357
200	3.752	2.60	2.69	2.36	0.385	0.0508	0.0189	0.00384
250	5.146	2.63	2.01	1.76	0.379	0.0534	0.0206	0.00416
300	7.211	2.66	1.48	1.32	0.391	0.0577	0.0227	0.00443
350	10.02	2.67	1.10	0.99	0.360	0.0597	0.0233	0.00475
400	12.81	2.75	0.87	0.75	0.337	0.0636	0.0250	0.00498
450	17.15	2.83	0.67	0.56	0.305	0.0667	0.0269	0.00526
500	23.28	2.84	0.51	0.43	0.261	0.0689	0.0282	0.00563
550	31.71	2.87	0.39	0.32	0.218	0.0696	0.0291	0.00588
600	43.38	2.88	0.30	0.24	0.177	0.0671	0.0304	0.00629
650	59.58	2.91	0.24	0.18	0.141	0.0633	0.0311	0.00660

[a] Errors were within 2%. [b] Errors were estimated from the plots of $1/\tau$ versus [Q] except for BE (within 5%). [c] Reference 13 for data at the pressures of up to 400 MPa. [d] See text.

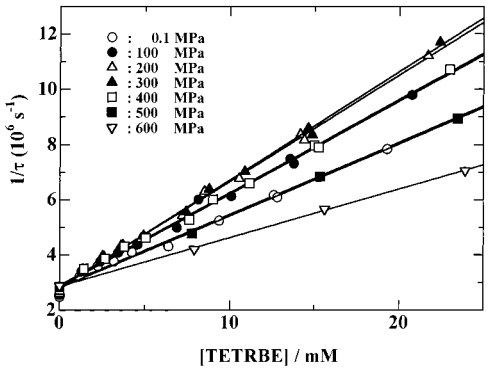

Figure 1. Plots of $1/\tau$ versus the concentration of TETRBE, [TETRBE], in MCH at 25 °C.

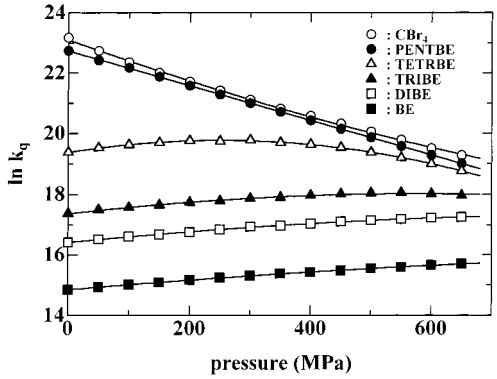

Figure 2. Pressure dependence of k_q in MCH at 25 °C.

slope of the plot of the inverse of the lifetime, τ^{-1}, versus [Q], according to

$$1/\tau - 1/\tau_0 = k_q[Q] \tag{2}$$

where τ_0 is the lifetime in the absence of Q. Figure 1 shows the plots of $1/\tau$ versus [Q] for TETRBE. The values of k_q are listed in Table 2 for six quenchers in MCH at the pressures of up to 650 MPa. In Table 2, the data for CBr_4 at the pressures of up to 400 MPa are those reported in the previous publication.[13]

The quenching for BE was carried out in bulk solution because of the low k_q. The lifetime decreased from 25.3 to 8.71 ns on going from 0.1 to 650 MPa at 25 °C. The lifetime at 0.1 MPa is significantly smaller and its pressure dependence is larger compared with the results in MCH (see Table 2). Clearly, the short lifetime and its larger pressure dependence in BE may result in the heavy-atom quenching by BE. The values of k_q determined by assuming that τ_0(BE) $\sim$ τ_0(MCH) (eq 2) are also listed in Table 2.

The plot of ln k_q versus pressure is shown in Figure 2. For CBr_4 and PENTBE, k_q decreases significantly in the whole pressure range, whereas it increases moderately for TETRBE and TRIBE and then decreases with increasing pressure. Furthermore there is a monotonical increase in k_q for DIBE and BE. The activation volume, $\Delta V_q^{\ddagger}$, at 0.1 MPa was determined from the pressure dependence of k_q according to eq 3, where κ is the isothermal compressibility of the solvent.

$$RT(\partial \ln k_q/\partial P)_T = -\Delta V_q^{\ddagger} - RT\kappa \tag{3}$$

The values of $\Delta V_q^{\ddagger}$ are summarized in Table 3, where it is noted that the activation volume is positive for CBr_4 and PENTBE with high k_q values, whereas it is negative for the other quenchers with k_q values of $\sim 10^6 - 10^8$ M^{-1} s^{-1} at 0.1 MPa.

TABLE 3: Activation Volumes (cm^3/mol) in MCH at 0.1 MPa and 25 °C

quencher	$\Delta V_q^{\ddagger}$	$\Delta V_{diff}^{\ddagger(HS)} - \Delta V_{-diff}^{\ddagger(HS)}$	$\Delta V_{q\gamma}^{\ddagger}$
CBr_4	18.9 ± 0.7	-9.4 ± 0.4	23.8 ± 0.7
PENTBE	12.0 ± 0.4	-9.5 ± 0.4	20.1 ± 0.3
TETRBE	-10.2 ± 0.4	-9.5 ± 0.4	1.0 ± 0.2
TRIBE	-8.0 ± 0.6	-9.4 ± 0.4	0.8 ± 0.1
DIBE	-7.3 ± 0.4	-9.3 ± 0.4	0.3 ± 0.1
BE	-7.1 ± 0.4	-9.2 ± 0.4	1.1 ± 0.2

Discussion

Rate Constant for Diffusion. In general, when the transient terms can be neglected, the rate constant, k_{diff}, for the bimolecular diffusion-controlled reaction between $^1M^*$ and Q is given by eq 4 in a solvent with the relative diffusion coefficient, D_{M^*Q} ($= D_{M^*} + D_Q$):[20,21]

$$k_{diff} = 4\pi r_{M^*Q} D_{M^*Q} N_A/10^3 \tag{4}$$

where r_{M^*Q} and N_A are the encounter distance and Avogadro's number, respectively. The relationship between D_i (i = M* or Q) and ζ_i, the friction coefficient, for the solute molecule, i, in a given solvent is expressed by the Einstein equation, $D_i = k_B T/\zeta_i$, where k_B is the Boltzmann constant. Because the hydrodynamic friction, ζ_i^H, for the solute molecule of the spherical radius, r_i, in a continuum medium with viscosity, η, is given by $\zeta_i^H = \pi f_i r_i \eta$ (Stokes' Law), one can obtain the Stokes−Einstein (SE) equation,

$$D_i^{SE} = k_B T/\pi f_i r_i \eta \tag{5}$$

where f_i = 6 and 4 for the stick and slip boundary limits, respectively. However, the SE equation has often been observed to break down for diffusion in liquid solution.[20,33,34]

In the previous publication,[13,27] the solvent-viscosity dependence of k_{diff} induced by pressure was described successfully for several quenching systems on the basis of an empirical equation proposed by Spernol and Wirtz.[22,23] According to their approach, the diffusion coefficient, D_i^{SW}, is expressed by

$$D_i^{SW} = k_B T/6\pi f_i^{SW} r_i \eta \tag{6}$$

where f_i^{SW} represents a microfriction factor and is given by

$$f_i^{SW} = (0.16 + 0.4 r_i/r_s)(0.9 + 0.4 T_S^r - 0.25 T_i^r) \tag{7}$$

In eq 7, the first parenthetical quantity depends only on the solute-to-solvent size ratio, r_i/r_S (see Table 1). The second parenthetical quantity involves the reduced temperatures, T_S^r and T_i^r, of solvent and solute, respectively, which can be calculated with the melting point, T_{mp}, and boiling point, T_{bp}, of the solvent or solute (Table 1) at the experimental temperature, T, according to

$$T_{i(S)}^r = [T - T_{mp(S)}]/[T_{bp(S)} - T_{mp(S)}] \tag{8}$$

From the approximation by Spernorl and Wirtz, eq 9 can be derived

$$k_{diff} = \frac{2RTr_{M^*Q}}{3000\eta}\left(\frac{1}{f_{M^*}^{SW} r_{M^*}} + \frac{1}{f_Q^{SW} r_Q}\right) \tag{9}$$

TABLE 4: Values of α^{SW}, α^{ex}, and k_{bim} in MCH

	α^{SW}			
quencher	trunc	full	α^{ex}	k_{bim}, 10^{10} M^{-1} s^{-1}
CBr_4	1710	2260	$1740 \pm 20^{a,b}$	$2.5 \pm 0.3^{a,b}$
			1760 ± 20^{c}	1.9 ± 0.4^{c}
PENTBE	1800	2260	1860 ± 20^{b}	1.0 ± 0.3^{b}
			1954 ± 20^{c}	1.1 ± 0.3^{c}
TETRBE	1760	2120	1780 ± 10^{b}	0.058 ± 0.003^{b}
			1929 ± 20^{c}	0.028 ± 0.001^{c}
TRIBE	1710	2010		
DIBE	1640	1960		
BE	1560	1620		

[a] Reference 13. [b] The values of α^{ex} and k_{bim} were evaluated by the plots of $1/k_q$ versus η (see eq 12). [c] The values of α^{ex} and k_{bim} were evaluated by the plots of γ/k_q versus $\gamma\eta$ (see eq 17).

By comparing with eq 1, α^{SW} is given by

$$\alpha^{SW} = \frac{1.2 \times 10^4}{r_{M^*Q}}\left(\frac{1}{f_{M^*}^{SW} r_{M^*}} + \frac{1}{f_{Q}^{SW} r_{Q}}\right)^{-1} \qquad (10)$$

The values of f_i at 0.1 MPa for the solute−MCH systems examined in this study are listed in Table 1, where f_i^{SW} (full) and f_i^{SW} (trunc) were evaluated by eq 7 and by neglecting the second parenthetical quantity in eq 7, respectively.[35]

Available experimental data indicate that self-diffusion coefficients are approximately inversely proportional to the pressure-induced solvent viscosity, η, for a number of liquids.[31,36] The value of f_i^{SW} evaluated according to eq 7 is 0.42 for MCH, which is smaller by ∼30% than the values listed in Table 1, but the agreement between experimental and calculated values is fairly good. Unfortunately, there are no data available of mutual diffusion coefficients in MCH at high pressures. Dymond and Woolf measured the diffusion coefficients of benzene, toluene, and benzo[*a*]pyrene in *n*-hexane at the pressures of up to 384 MPa and 25 °C.[37] The diffusion coefficients are approximately inversely proportional to the pressure-induced solvent viscosity, η. The values of f_i^{SW} evaluated from their data are 0.50, 0.51, and 0.65 for benzene, toluene, and benzo[*a*]pyrene, respectively; these values are in good agreement with those of f_i^{SW} calculated according to eq 7; f_i^{SW}(trunc) = 0.52, 0.54, and 0.66, and f_i^{SW}(full) = 0.58, 0.57, and 0.86 for benzene, toluene, and benzo[*a*]pyrene, respectively.[38]

The values of α^{SW} calculated by eq 10 for the quenching systems studied in this work are shown in Table 4. As seen in Table 4, α^{SW}(trunc) and α^{SW}(full) are close to the value for the slip boundary limit ($\alpha = 2000$) rather than that for the stick boundary limit ($\alpha = 3000$).

Solvent Viscosity Dependence of k_q. The mechanism of the fluorescence quenching by the heavy-atom quenchers examined in this work should be explained in the same framework. It was reported in the previous publication[13] that the quenching occurs via an exciplex, (MQ)*, which is formed from an encounter complex, $(M^*Q)_{en}$, between the excited singlet state of PY (M^*) and heavy-atom quencher (Q) in the solvent cage, as shown in Scheme 1, where the bar indicates the solvent cage. According to the mechanism shown in Scheme 1, the observed rate constant, k_q, is given by

$$k_q = \frac{k_{diff}}{1 + k_{-diff}\left(\frac{k_p + k_{-c}}{k_c k_p}\right)} \qquad (11)$$

When the rate constant for diffusion, k_{diff}, is expressed by eq 1

SCHEME 1

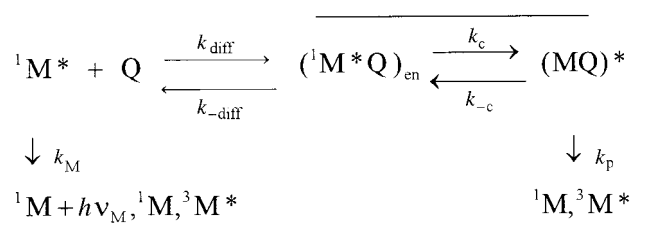

(α is replaced by α^{ex}), one may derive eq 12 from eqs 1 and 11:

$$\frac{1}{k_q} = \left(\frac{k_p + k_{-c}}{k_c k_p}\right)\left(\frac{k_{-diff}}{k_{diff}}\right) + \frac{\alpha^{ex}}{8RT}\eta \qquad (12)$$

In the previous work,[13] the fluorescence quenching by CBr_4 of 1,2-benzanthracene and PY was examined at pressures of up to 400 MPa. It was found that the plot of $1/k_q$ versus η is linear, and it was concluded that the bimolecular rate constant for the quenching, k_{bim}, defined by $k_c k_{diff}/k_{-diff}$, is independent of pressure. Here, we redefine k_{bim} by eq 13 according to eq 12:

$$k_{bim} = \left(\frac{k_c k_p}{k_p + k_{-c}}\right)\left(\frac{k_{diff}}{k_{-diff}}\right) \qquad (13)$$

When one assumes that $k_p \gg k_{-c}$ in eq 13, then k_{bim} is equal to $k_c k_{diff}/k_{-diff}$, which is in agreement with the previous definition of k_{bim} for the quenching by CBr_4.[13] The values of k_{bim} and α^{ex} for CBr_4 evaluated previously[13] are listed in Table 4, together with those for the other quenching systems discussed later.

Figure 3 shows the plots of $1/k_q$ versus η for six quenchers. The plot for CBr_4 in Figure 3a, in which the data are extended to the pressures of up to 650 MPa in this work and where η increases ∼90 times, shows slight downward curvature. The mean values of α^{ex}, determined from the slope of the plot of $1/k_q$ versus η, decreased from 1730 (0.1−400 MPa) to 1310 (400−650 MPa). This decrease implies that k_{diff} deviates slightly from the $1/\eta$ dependence in the wide viscosity range, although the pressure dependence of α^{ex} is not significant. As a result, in agreement with the conclusion described in the previous work, the quenching by CBr_4 is competing with diffusion at the lower pressure region and approaches a diffusion-controlled process as pressure increases further.

For PENTBE, the plot shown in Figure 3a is almost linear, leading probably to the same conclusion as for the quenching by CBr_4. The values of k_{bim} and α^{ex} that are determined from the least-squares intercept and slope of the plot of $1/k_q$ versus η (Figure 3a), respectively, are listed in Table 4. The value of α^{ex} in Table 4 is close to that of α^{SW} (trunc), indicating that the estimation of k_{diff} by eq 12 is valid.

For TETRBE and TRIBE, one can find a minimum in the plot of $1/k_q$ versus η, which is shown in Figures 3a and 3b. It is noted in Figures 3a and 3b that the plots increase linearly at pressures above ∼450 MPa for TETRBE and ∼550 MPa for TRIBE. From the linear portion of the plots, the values of α^{ex} were estimated to be 1780 (TETRBE) and 1100 (TRIBE); the value of α^{ex} for TETRBE is in good agreement with that of α^{SW} (trunc) (Table 4). This agreement means that the quenching by TETRBE is diffusion controlled in the higher viscosity region. Consequently, this fact suggests that the minimum observed in the plot of $1/k_q$ versus η arises as a result of a decrease in k_{diff} and an increase in the bimolecular quenching constant, k_{bim} (eq 13), with increasing pressure.

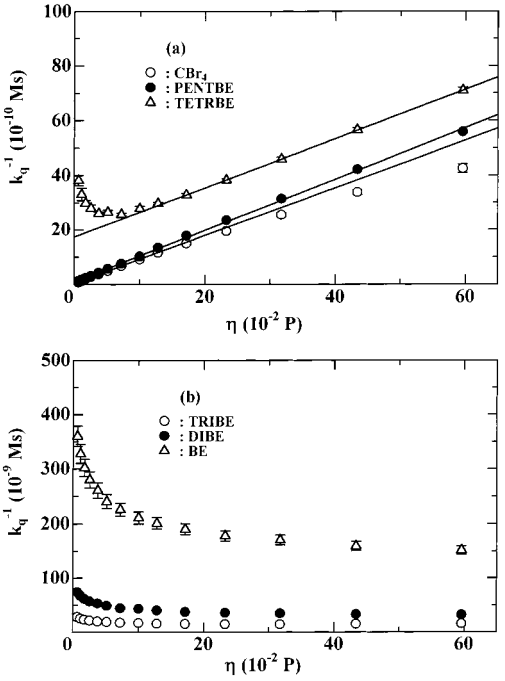

Figure 3. Plots of $1/k_q$ versus η in MCH at 25 °C.

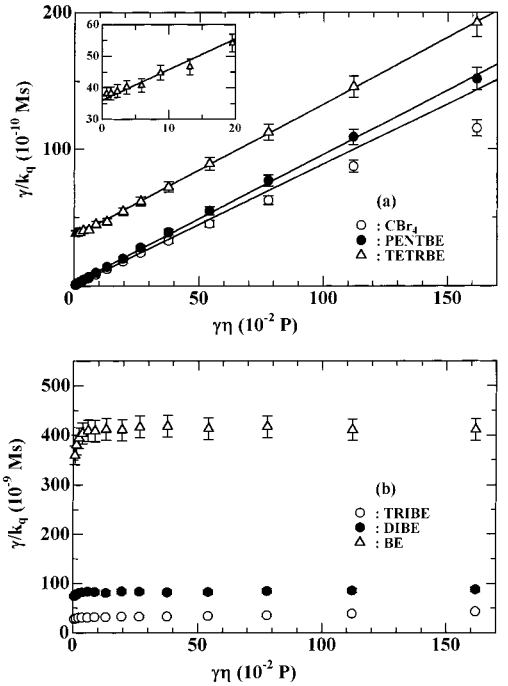

Figure 4. Plots of γ/k_q versus $\gamma\eta$ in MCH at 25 °C.

The increase in k_{bim} with increasing pressure can be clearly observed for DIBE and BE (Figures 2) with lower quenching ability for which k_{bim} is much smaller than k_{diff} calculated by using α^{SW} and η according to eq 1. We discuss the reasons why k_{bim} increases with increasing pressure in liquid solution next.

Pressure Dependence of k_{bim}. For the fluorescence quenching by the quenchers with low k_q, k_{bim}, defined by eq 13, increases with increasing pressure as mentioned in the previous section. For the strong quenchers, CBr_4 and PENTBE for which k_p is much larger than k_{-c} ($k_p \gg k_{-c}$), k_{bim} ($= k_c k_{diff}/k_{-diff}$) is also expected to increase with increasing pressure; but, no pressure dependence was observed. Probably, the increase of k_{bim} is buried in the significant decrease of k_{diff} with increasing pressure because k_{bim} is comparable to k_{diff} at 0.1 MPa (see Table 4). Thus, the plot of $1/k_q$ versus η is linear and the intercept giving k_{bim} is apparently independent of pressure, as pointed out in the previous work.[13]

It was reported that the lifetime of singlet oxygen in liquid solution decreases moderately with increasing pressure, and the pressure dependence was satisfactorily interpreted by that of the radial distribution function at the closest approach distance of the solute and solvent molecules.[14,15] In a hard sphere solution consisting of a hard-sphere PY molecule with a radius of r_{M^*} and a hard-sphere heavy-atom quencher molecule with a radius of r_Q in a hard-sphere solvent molecule with a radius of r_S, the volume change, $\Delta V_{diff}^{\ddagger(HS)} - \Delta V_{-diff}^{\ddagger(HS)}$ for the encounter complex formation is given by[39]

$$\Delta V_{diff}^{\ddagger(HS)} - \Delta V_{-diff}^{\ddagger(HS)} = -RT\left[\frac{\partial \ln g(r_{M^*Q})}{\partial P}\right]_T - RT\kappa \quad (14)$$

where $g(r_{M^*Q})$, the radial distribution function at the closest approach distance (the encounter distance), $r_{M^*Q}(= r_{M^*} + r_Q)$, is expressed by

$$g(r_{M^*Q}) = \frac{1}{1-y} + \frac{3y}{(1-y)^2}\left(\frac{r_{red}}{r_S}\right) + \frac{2y^2}{(1-y)^3}\left(\frac{r_{red}}{r_S}\right)^2 \quad (15)$$

and κ is the isothermal compressibility of solvent. In eq 15, r_{red} $= r_{M^*}r_Q/r_{M^*Q}$, and y is the packing fraction, given in terms of the molar volume of solvent, V_S, by

$$y = \frac{4N_A\pi r_S^3}{3V_S} \quad (16)$$

By using the values of r_S, r_{M^*}, and r_Q listed in Table 1,[40] together with the data of the solvent density,[29−31] $\Delta V_{diff}^{\ddagger(HS)} - \Delta V_{-diff}^{\ddagger(HS)}$ was determined from eq 14. The results are summarized in Table 3. It is noted in Table 3 that the value of $\Delta V_{diff}^{\ddagger(HS)} - \Delta V_{-diff}^{\ddagger(HS)}$ is negative and almost independent of the quenchers examined, and also approximately equal to $\Delta V_q^{\ddagger}$ for the quenchers with low k_q. This result suggests that the pressure dependence of k_{bim} is attributed to that of k_{diff}/k_{-diff} (see eq 13).

According to eq 14, the ratio of k_{diff}/k_{-diff} at P MPa to that at 0.1 MPa, $(k_{diff}/k_{-diff})_P/(k_{diff}/k_{-diff})_0$, is expressed by $g(r_{M^*Q})_P/g(r_{M^*Q})_0$. Therefore, one can obtain eq 17 from eq 12.

$$\frac{\gamma}{k_q} = \left(\frac{k_p + k_{-c}}{k_c k_p}\right)\left(\frac{k_{-diff}}{k_{diff}}\right)_0 + \frac{\alpha^{ex}}{8RT}\eta\gamma \quad (17)$$

where

$$\gamma = g(r_{M^*Q})_P/g(r_{M^*Q})_0$$

Plots of γ/k_q versus $\gamma\eta$ for six quenchers are shown in Figure 4, where the plot for CBr_4 was drawn with data at pressures up to 400 MPa because k_{diff} deviates slightly from the $1/\eta$ dependence in the wide viscosity range, as already mentioned. In Figure 4, γ/k_q increases linearly with a positive intercept as $\gamma\eta$ increases for PENTBE and TETRBE, but is almost independent of $\gamma\eta$ for TRIBE, DIBE, and BE. It is also seen in Figure 4 that the plot of γ/k_q versus $\gamma\eta$ for TETRBE is approximately linear, although the plot of $1/k_q$ versus η has a minimum (Figure 3), strongly suggesting the validity of eq 17. The values of α^{ex} and k_{bim}, determined from the least-squares slopes and intercepts of the linear plots in Figure 4, respectively, for CBr_4, PENTBE, and TETRBE are listed in Table 4.[41] For CBr_4 and PENTBE, the values of α^{ex} and k_{bim} are roughly equal

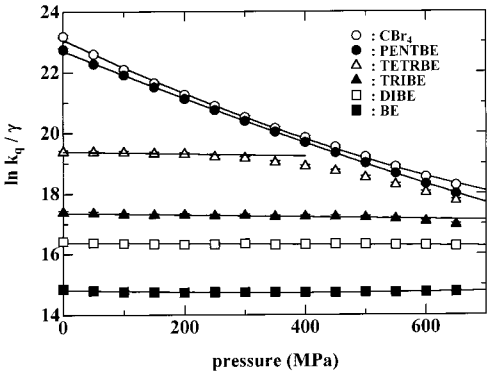

Figure 5. Pressure dependence of k_q/γ in MCH at 25 °C.

to those evaluated by eq 12. However, the value of k_{bim} for TETRBE is significantly smaller than that determined by eq 12, although the difference in α^{ex} is not large. For CBr_4 and PENTBE, k_{bim} is comparable to k_{diff} at 0.1 MPa, so the observed k_q rapidly approaches k_{diff} because k_{bim} increases moderately, whereas k_{diff} decreases significantly with increasing pressure. This situation may lead to almost no difference in k_{bim}. For TETRBE, on the other hand, k_{bim} is much smaller than k_{diff} at 0.1 MPa, and hence the observed k_q gradually approaches the region where k_{bim} competes with k_{diff} with increasing pressure. Thus, the large difference in k_{bim} determined by eqs 12 and 17 for TETRBE (Table 4) may be understood.

According to eq 17, in the region where k_{bim} does not compete with k_{diff}, γ/k_q should be independent of $\gamma\eta$. In fact, the plots for TRIBE, DIBE and BE, which are shown in Figure 4b, are approximately independent of $\gamma\eta$, although they increase very slightly in the low $\gamma\eta$ region. Figure 5 shows plots of $\ln(k_q/\gamma)$ against pressure to confirm the validity of eq 17 further.[41] As seen in Figure 5, k_q/γ for DIBE and BE is almost independent of pressure at the whole pressure range examined. It can be also seen in Figure 5 that the plots indicate no significant contribution of diffusion at the pressure below ~200 and ~500 MPa for TETRBE and TRIBE, respectively. The apparent activation volume for four quenchers at 0.1 MPa, $\Delta V_{q\gamma}^{\ddagger}$, which is listed in Table 3, is nearly zero, also supporting the validity of eq 17. Thus, it may be concluded that the pressure dependence of k_q for the quenchers with the low quenching ability is described satisfactorily by that of the radial distribution function of the closest approach distance with a hard sphere assumption. This conclusion may be also valid for the quenchers with high quenching ability, CBr_4 and PENTBE.

Finally, the linear plot of γ/k_q versus $\gamma\eta$ (eq 17) means that $k_c k_p/(k_p + k_{-c})$ is independent of pressure. For CBr_4 and PENTBE ($k_p \gg k_{-c}$), k_c may be independent of pressure. This situation is probably valid for the other quenching systems examined in this work. The evidence, together with the fact that the rate constant for the decay process of excimer and exciplex, k_p, is approximately independent of pressure in nonpolar solvent,[13, 32] suggests that k_{-c} is independent of pressure. For the typical exciplex systems, it was found that k_{-c} decreases significantly with increasing pressure, and the positive activation volume was interpreted in terms of the bond cleavage and the loss of solvation involved in the dissociation process of the exciplexes.[13] The present finding that k_{-c} is independent of pressure implies that the interaction between M* and Q to form an exciplex is weak.

Conclusion

The fluorescence quenching of PY by six heavy-atom quenchers in MCH at pressures up to 650 MPa and 25 °C has been examined. The pressure dependence of the quenching rate constant, k_q, shows a monotonical decrease, a maximum, and a monotonical increase, depending on the heavy-atom quencher examined. The observations have been interpreted by a mechanism that involves formation of an encounter complex followed by the formation of an exciplex between M* and Q (see Scheme 1). Analysis based on this mechanism has revealed that the quenching involves both contributions of the bimolecular rate constant, k_{bim}, defined by eq 13 and the rate constant for diffusion, k_{diff}, that is inversely proportional to the solvent viscosity (eq 1). The evidence, together with the experimental results, has led to a conclusion that k_{bim} may increase with increasing pressure. The ratio, k_{diff}/k_{-diff}, involved in k_{bim} was calculated on the basis of the radial distribution function, $g(r_{M^*Q})$, at the closest approach distance between M* and Q with a hard sphere assumption, and it was found that the pressure dependence of k_{diff}/k_{-diff} is approximately equal to that of k_{bim}. Therefore, the pressure dependence of k_{bim}, with negative activation volume, was attributed to that of k_{diff}/k_{-diff}. An equation that can be applied to the fluorescence quenching by the heavy-atom quenchers with nearly diffusion-controlled rate has been proposed.

References and Notes

(1) McGlynn, S. P.; Azumi, T.; Kinoshita, M. *Molecular Spectroscopy of the Triplet State*; Prentice-Hall: Englewood Cliffs, NJ, 1969; Chapter 8.
(2) Birks, J. B. *Photophysics of Aromatic Molecules*; Wiley-Interscience: New York, 1970; Chapter 9.
(3) Bowen, E. J.; Metcalf, W. S. *Proc. R. Soc. A* **1951**, *206*, 437.
(4) Melhuish, H. W.; Metcalf, W. S. *J. Chem. Soc.* **1954**, 976.
(5) Melhuish, H. W.; Metcalf, W. S. *J. Chem. Soc.* **1958**, 480.
(6) Thomaz, M. F.; Stevens, B. *Molecular Luminescence*; Lim, E., Ed.; Benjamin: New York, 1969; p 153.
(7) Shimizu, Y.; Azumi, T. *J. Phys. Chem.* **1982**, *86*, 22.
(8) Ware, W. R.; Novros, J. S. *J. Phys. Chem.* **1966**, *70*, 3246.
(9) Nemzek, T. M.; Ware, W. R. *J. Chem. Phys.* **1975**, 62, 477.
(10) Haworth, D. W.; Metcalf, W. S. *J. Chem. Soc.* **1965**, 4678.
(11) Ewald, A. H. *J. Phys. Chem.* **1963**, *67*, 1727.
(12) Okamoto, M.; Teranishi, H. *J. Phys. Chem.* **1984**, *88*, 5644.
(13) Okamoto, M. *J. Phys. Chem. A* **2000**, *104*, 5029.
(14) Okamoto, M.; Tanaka, F.; Teranishi, H. *J. Phys. Chem.* **1990**, *94*, 669.
(15) Schmidt, R.; Seikel, K.; Brauer, H.-D. *Ber. Bunsen-Ges. Phys. Chem.* **1990**, *94*, 1100.
(16) Okamoto, M.; Tanaka, F. *J. Phys. Chem.* **1993**, *97*, 177.
(17) Seikel, K.; Brauer, H−D. B*er. Bunsen-Ges. Phys. Chem.* **1991**, *95*, 900.
(18) Hild, M.; Brauer, H.-D. *Ber. Bunsen-Ges. Phys. Chem.* **1996**, *100*, 1210.
(19) Okamoto, M. *J. Photochem. Photobiol. A Chemistry* **1999**, *124*, 113.
(20) Birks, J. B. *Organic Molecular Photophysics*; Wiley: New York, 1973; p 403.
(21) Rice, S. A. In *Comrehensive Chemical Kinetics. Diffusion-Limited Reactions*; Bamford, C. H., Tripper, C. F. H., Compton, R. G., Eds.; Elsevier: Amsterdam, 1985; Vol 25.
(22) Spernol, A.; Wirtz, K. *Z. Naturforsch.* **1953**, *8A*, 522.
(23) Gierer, A.; Wirtz, K. *Z. Naturforsch.* **1953**, *8A*, 532.
(24) Schuh, H.-H.; Fischer, H. *Helv. Chim. Acta* **1978**, *61*, 2130.
(25) Saltiel, J.; Atwater, B. W. *Advances in Photochemistry*; Wiley-Interscience: New York, 1987; Vol 14, p 1.
(26) Saltiel, J.; Shannon, P. T.; Zafiriou, O. C.; Uriarte, K. *J. Am. Chem. Soc.* **1980**, *102*, 6799.
(27) Okamoto, M. *J. Phys. Chem. A* **1998**, *102*, 4751.
(28) Bondi, A. *J. Phys. Chem.* **1964**, *68*, 441.
(29) Bridgman, P. W. *Proc. Am. Acad. Arts. Sci.* **1926**, *61*, 57.
(30) Brazier, D. W.; Freeman, G. R. *Can. J. Chem.* **1969**, *47*, 893.
(31) Jonas, J.; Hasha, D.; Huang, S. G. *J. Chem. Phys.* **1979**, *71*, 3996.
(32) Okamoto, M.; Sasaki, M. *J. Phys. Chem.* **1991**, *95*, 6548.
(33) Evance, D. F.; Tominaga, T.; Chan, C. *J. Solution Chem.* **1979**, *8*, 461.
(34) Evance, D. F.; Tominaga, T.; Davis, H. T. *J. Chem. Phys.* **1981**, *74*, 1298.
(35) Because the values of the critical temperature, T_c, pressure, P_c, and volume, V_c, for MCH are 572.2 K, 3.47 MPa, and 368 cm^3/mol, respectively, T_{bp}(s) in eq 8 is not evaluated at pressures $> P_c$.
(36) As a review article; Jonas, J. *Acc. Chem. Res.* **1984**, *17*, 74.

(37) Dymond, J. H.; Woolf, L. A. *J. Chem. Soc., Faraday Trans. 1* **1982**, *78*, 991.

(38) The values of van der Waals radii were estimated to be 0.268, 0.287, 0.374, and 0.301 nm for benzene, toluene, benzo[*a*]pyrene, and *n*-hexane, respectively, according to the method of Bondi.[28]

(39) Yoshimura, Y.; Nakahara, M. *J. Chem. Phys.* **1984**, *81*, 4080.

(40) The isothermal compressibility of the hard-sphere liquid, $\kappa^{(HS)}$, is expressed by[39]

$$\kappa^{(HS)} = \frac{V_S(1-y)^4}{RT(1+4y+4y^2-4y^3+y^4)} \qquad \text{(A1)}$$

The packing fraction, y, was estimated by equating $\kappa^{(HS)}$ to the observed isothermal compressibility, κ,[29−31] for MCH, and r_S was evaluated as 0.292 nm according to eq A1. The value of r_S thus evaluated is smaller by ∼3% than that estimated according to the method of Bondi.[28] Therefore, the value of r_S calculated by the method of Bondi (Table 1) was used for analysis.

(41) The plot of γ/k_q versus $\gamma\eta$ leads to a large error for determination of the intercept. Therefore, the values of α^{ex} and k_{bim} were also evaluated by the nonlinear least-squares method according to the equation, $k_q/\gamma = k_{bim}^0/(1 + A\gamma\eta)$ (see eq 17), where k_{bim}^0 represents k_{bim} at 0.1 MPa and $A = \alpha^{ex}k_{bim}^0/8RT$: $\alpha^{ex} = 2040 \pm 210$ and $k_{bim}^0 = (6.1 \pm 0.6) \times 10^{10}$ M^{-1} s^{-1} for CBr_4 (0.1−400 MPa): $\alpha^{ex} = 2160 \pm 115$ and $k_{bim}^0 = (1.7 \pm 0.1) \times 10^{10}$ M^{-1} s^{-1} for PENTBE (0.1−650 MPa); and $\alpha^{ex} = 1840 \pm 60$ and $k_{bim}^0 = (0.027 \pm 0.001) \times 10^{10}$ M^{-1} s^{-1} for TETRBE (0.1−650 MPa). The values thus evaluated are in good agreement with those listed in Table 4.